microRNAs involved in auxin signalling modulate male sterility under high-temperature stress in cotton (*Gossypium hirsutum*)

Yuanhao Ding, Yizan Ma, Nian Liu, Jiao Xu, Qin Hu, Yaoyao Li, Yuanlong Wu, Sai Xie, Longfu Zhu, Ling Min* and Xianlong Zhang

National Key Laboratory of Crop Genetic Improvement, Huazhong Agricultural University, Wuhan 430070, China

SUMMARY

Male sterility caused by long-term high-temperature (HT) stress occurs widely in crops. MicroRNAs (miR-NAs), a class of endogenous non-coding small RNAs, play an important role in the plant response to various abiotic stresses. To dissect the working principle of miRNAs in male sterility under HT stress in cotton, a total of 112 known miRNAs, 270 novel miRNAs and 347 target genes were identified from anthers of HT-insensitive (84021) and HT-sensitive (H05) cotton cultivars under normal-temperature and HT conditions through small RNA and degradome sequencing. Quantitative reverse transcriptase-polymerase chain reaction and 5′-RNA ligase-mediated rapid amplification of cDNA ends experiments were used to validate the sequencing data. The results show that miR156 was suppressed by HT stress in both 84021 and H05; miR160 was suppressed in 84021 but induced in H05. Correspondingly, *SPLs* (target genes of miR156) were induced both in 84021 and H05; *ARF10* and *ARF17* (target genes of miR160) were induced in 84021 but suppressed in H05. Overexpressing miR160 increased cotton sensitivity to HT stress seen as anther indehiscence, associated with the suppression of *ARF10* and *ARF17* expression, thereby activating the auxin response that leads to anther indehiscence. Supporting this role for auxin, exogenous Indole-3-acetic acid (IAA) leads to a stronger male sterility phenotype both in 84021 and H05 under HT stress. Cotton plants overexpressing miR157 suppressed the auxin signal, and also showed enhanced sensitivity to HT stress, with microspore abortion and anther indehiscence. Thus, we propose that the auxin signal, mediated by miRNAs, is essential for cotton anther fertility under HT stress.

Keywords: *Gossypium hirsutum*, male sterility, high-temperature stress, miRNA sequencing, degradome sequencing, miRNAs, auxin signal, miR156/157, miR160.

INTRODUCTION

Under climate change, high-temperature (HT) stress has become a serious threat to crop yield due to its negative effects on plant development and reproduction (Bita and Gerats, 2013). Male sterility caused by HT has been known for decades to reduce yield in several crops, such as rice, wheat, corn, rapeseed and cotton (Xing *et al.*, 2003; Tang *et al.*, 2006; Chen *et al.*, 2007; Zhi *et al.*, 2007; Zeng *et al.*, 2014). At the same time, temperature (thermo)-sensitive genic male sterility (TGMS) has been used as a powerful tool for hybrid breeding, but little is known about the mechanisms (Chen and Liu, 2014). The dissection of the molecular mechanism of male sterility under HT stress will therefore be helpful in the longer term for increasing crop productivity and promoting TGMS utilization in hybrid seed development.

Microsporogenesis and microgametogenesis are both extremely vulnerable to various environmental stresses (De Storme and Geelen, 2014). The microspore stage is especially sensitive to HT stress in several plant species, such as wheat, rice, cowpea and tomato (Bingham, 1966; Saini *et al.*, 1984; Namuco and O'Toole, 1986; Ahmed *et al.*, 1992; Kim *et al.*, 2001; Sato *et al.*, 2002; Endo *et al.*, 2009). Anther indehiscence, microspore abortion, rudimentary pollen tube formation and premature degeneration of the tapetum all occur during HT stress (Paupiere *et al.*, 2014). Molecular changes in the basic thermotolerance response to HT stress have been documented in plants, including heat shock factor and heat shock protein responses, reactive oxygen species (ROS) signalling and calcium signalling pathways (Bokszczanin *et al.*, 2013). In

addition, endogenous phytohormones such as auxin, gibberellin acid (GA) and jasmonate (JA) have been reported to participate in the response to HT stress during anther development (Chhun *et al.*, 2007; Sakata *et al.*, 2010; Cecchetti *et al.*, 2013).

Previously we showed that overexpression of *Gossipium hirsutum CASEIN KINASEI* (*GhCKI*) delayed normal programmed cell death (PCD) in the tapetum and resulted in anther abortion and indehiscence, and earlier expression of *GhCKI* was induced by HT in the HT-sensitive cotton line (Min *et al.*, 2013). We also proposed that *PHYTOCHROME-INTERACTING FACTOR* (*PIF*) genes induced by sugar signalling positively promote indole-3-acetic acid (IAA) biosynthesis and ultimately lead to male sterility of cotton under HT stress (Min *et al.*, 2014). However, HT stress was reported to suppress auxin biosynthesis and cause male sterility in barley and Arabidopsis, and the exogenous auxin can completely reverse male sterility under HT stress (Sakata *et al.*, 2010). Auxin perception mutants (*afb 1-3* and *tir1 afb2 afb3*) show earlier anther dehiscence and endothecium lignification by promoting JA signalling in Arabidopsis (Cecchetti *et al.*, 2013). Thus, auxin signalling can be assumed to play an important role in anther responses to HT stress, but the molecular mechanisms remain unclear.

MicroRNAs (miRNAs) are an extensive class of endogenous non-coding small RNAs involved in the plant response to biotic and abiotic stresses (Zhang, 2015). Many miRNAs have been detected in the plant response to HT stress through small RNA sequencing techniques in various species, including rice, wheat, barley and Arabidopsis (Zhao *et al.*, 2016). In the few miRNA functional analyses of plant responses to HT stress to date, miR398 is well studied. miR398 is rapidly induced by HT and makes the plant more sensitive to HT stress by repressing the expression level of copper superoxide dismutases, a class of important scavengers of ROS (Guan *et al.*, 2013). A second miRNA, miR156, plays a role in plant adaptation to recurring heat stress, and has been shown to be highly induced by HT in Arabidopsis (Kim *et al.*, 2012; Stief *et al.*, 2014). Other reports have demonstrated that miR160, miR166, miR167, miR172 and miR393, among others, are responsive to HT stress in plants (Kruszka *et al.*, 2014; Li *et al.*, 2014). Among these miRNAs, miR160, miR167 and miR393 are involved in the auxin signalling pathway, and their targets are auxin receptors or auxin response genes, such as *AUXIN F-BOX* (*AFB*), *TRANSPORT INHIBITOR RESISTANT 1* (*TIR1*) and *AUXIN RESPONSE FACTORS* (*ARFs*) (Sun, 2012). APETALA2-LIKE transcription factor (TF) RNAs, the target of miR172, function in the stress response and flower development (Wollmann *et al.*, 2010; Nova-Franco *et al.*, 2015). Although many miRNAs have been found to respond to HT stress, the mode of action of miRNAs in relation to male sterility remains unknown.

Our previous results have shown that epigenetic changes, such as genomic DNA methylation and histone modification, are involved in TGMS in cotton (Min *et al.*, 2014). miRNAs, as a form of epigenetic modification, were purported to take part in the process of TGMS in cotton. To identify the roles of miRNAs in TGMS in cotton, we used small RNA sequencing to detect miRNA changes during the development of male sterility in HT-sensitive (H05) and HT-insensitive (84021) cultivars. Degradome sequencing was then performed to identify the target genes of miRNAs. Among the detected miRNAs, miR157 and miR160 were overexpressed in cotton to elucidate their function during the cotton anther response to HT stress. Functional analysis revealed that miR160 regulates the expression of *ARFs* during anther indehiscence under HT stress. Overexpression of miR157 in cotton plants suppressed the expression level of *SPLs*, which caused a reduction in floral organ size and a highly increased sensitivity of anthers to HT stress. Our research reveals that miR160 and miR157 both regulate the auxin signalling pathway during the anther response to HT stress in cotton, to control male fertility.

RESULTS

Global small RNA analyses in anthers under normal-temperature (NT) and HT conditions

In our previous studies, two cotton lines, 84021 (HT-insensitive line) and H05 (HT-sensitive line), were employed to explore the mechanism of male sterility under HT stress at the transcript level, by RNA-Seq (Min *et al.*, 2013). Anther development was divided into 14 stages according to the length of the cotton bud planted in the field (Wu *et al.*, 2015). To illustrate the relationship between bud length and anther development in the greenhouse, a growth curve was made by measuring the bud length every day until flowering under normal conditions in the greenhouse (Figure S1). Anther development lasted nearly 25 days, from 3–4-mm buds (stage 4) to flowering. Because male sterility appears at 7–10 days after HT treatment in the greenhouse and considering the influence of HT on the progress of bud growth, the buds from 6–14 mm were deduced to be sensitive to HT stress. On this basis, buds of 6–7 mm (tetrad stage, TS) and 9–14 mm (tapetal degradation stage, TDS) were collected from H05 and 84021 under HT and control (NT) conditions, and used for small RNA and degradome sequencing to identify changes in miRNA abundance in response to HT stress.

Total RNA was extracted from 16 samples of two cultivars containing TS- and TDS-stage anthers of two biological replicates. Small RNA library construction and sequencing were performed by BGI in Shenzhen, China, using an Illumina HiSeq 2000 system. Nearly 12.3 million total reads were obtained from each sample after

removing poor-quality reads and adapter sequences (Figure 1a). Subsequently, sRNA lengths were counted, and the 17–29 nt distribution is shown in Figure 1b. All samples show the highest abundance at 24 nt and the second at 21 nt. Regarding 24 nt, siRNA is a class of small RNAs related to RNA-directed DNA methylation (Matzke and Mosher, 2014); the changes in the ratio of 24/21 nt might reflect changes in DNA methylation variation during anther development. Thus, the ratios of 24/21 nt sRNAs in each sample were compared. The results show that the ratio of 24/21 nt sRNAs at the TS was nearly twice as high as at the TDS (Figure 1c). sRNAs were then mapped to the cotton genome [*G. hirsutum* TM-1 (AD)1] to obtain annotations for repeats, introns, exons and up- and downstream sequences for each sRNA. The genome-mapping percentage of each sample is shown in Figure 1d. Similar

percentages of genome mappings were found between 84021 and H05 under NT conditions, but the percentages decreased from the TS to the TDS in both cultivars (82% at the TS, 72% at the TDS). During treatment with HT, all samples reached nearly 91% mapping regardless of the cultivars or the developmental stages.

Identification of known and candidate miRNAs in cotton anthers responding to HT stress

To identify the miRNAs in each sample, sRNAs were first annotated to remove irrelevant reads. The rRNAs, tRNAs, scRNAs, snRNAs and snoRNAs were then annotated by aligning the sRNAs to the GenBank and Rfam 11.0 databases, after which the sRNAs were removed, and the rest of the sRNAs were used to identify miRNAs according to the method described in the 'Bioinformatics analysis'
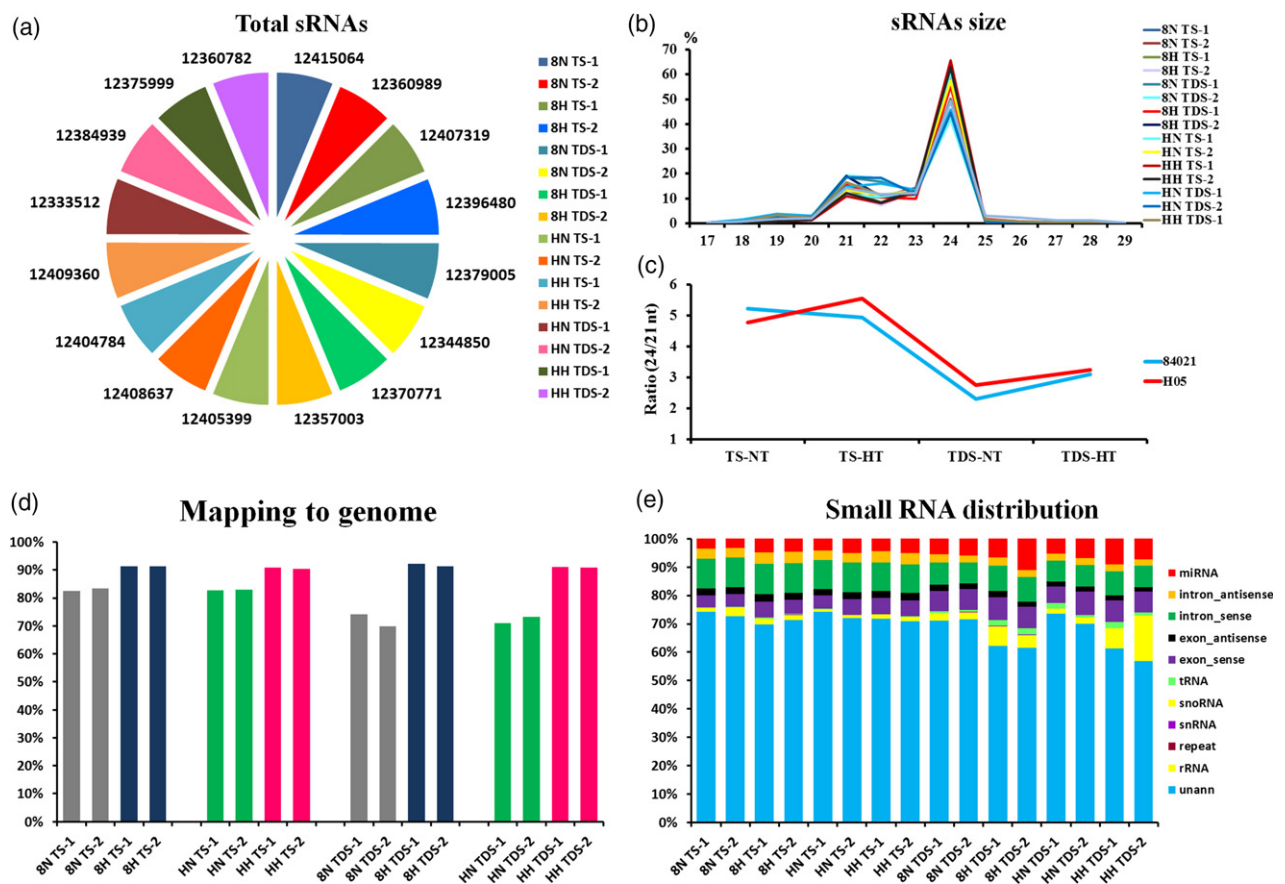

Figure 1. Small RNA sequencing quality and length distribution.
(a) Total sRNA reads distribution (ranging from 12 333 512 to 12 415 064) in 16 samples after removing poor-quality data.
(b) Length distribution of 17–29 nt small RNAs in 16 samples. All samples show highest abundance at 24 nt and second highest at 21 nt.
(c) The ratio of 24/21 nt sRNAs at the tetrad stage (TS) and tapetal degradation stage (TDS). The ratio at the TS is nearly twice that at the TDS in 84021 and H05 under both normal-temperature (NT) and high-temperature (HT) stress, and the ratio slightly increases under HT stress, except for 84021 at the TS. Two biological replicates were merged into mean value.
(d) The percentage of total sRNAs mapping to the cotton [*Gossypium hirsutum* TM-1 (AD)1] genome for each sample (Zhang *et al.*, 2015).
(e) The annotation distribution of the total sRNAs in each sample.
'8N TS-1': '8' represents the name of the cultivar '84021'; 'N' represents the treatment condition is normal temperature (NT); 'TS' represents that the bud development stage belongs to TS; and '-1' means 'the first biological repeat'. The meaning of other sample names can be deduced as illustrated above.

section of the 'Experimental Procedures' section. The final remaining sRNAs were labelled as unannotated sRNAs. Results showed that the unannotated sRNAs constituted the majority (56–74%); the sRNAs mapping to exons or introns made up nearly 17–23%; and the miRNAs made up nearly 5%. The remaining part (1~17%) was composed of rRNA, tRNA, scRNA, snRNA, snoRNA and repeats (Figure 1e). Finally, 112 known miRNAs and 270 novel miRNAs were detected from the small RNA sequencing analysis (Table S1).

To further classify the miRNAs, those with 20 or fewer reads in all samples were removed, leaving 83 known miR-NAs and 90 novel miRNAs (Table S1). The miRNAs were then screened with a higher stringency with transcripts per million (TPM) greater than 10 in at least one sample. This strategy produced 34 known miRNA families [18 conserved (can be found in other species) and 16 non-conserved (only found in cotton) families] and 23 novel miRNAs after merging the expression levels of each known miRNA family member together (Table S2). The two biological replicates were merged together by the mean value. We found that the highly abundant (TPM average > 100) conserved miRNA families were miR156/157, miR3954, miR166, miR172, miR168 and miR396. In addition, miR156/157 was the most abundant family, which makes up almost 63.71% of all conserved reads. On the other hand, miR8638, miR3476, miR7508 and miR7495 represent the highly abundant non-conserved miRNA families. The novel miRNAs exhibit mostly low abundance (TPM average < 58), consistent with the non-conserved or young miRNAs exhibiting lower expression than conserved miRNAs (Cuperus *et al.*, 2011). Interestingly, there were two2-fold more miRNA reads at the TDS than at the TS, regardless of whether the reads are in conserved or non-conserved miRNA families or whether they are novel miRNAs (Table S2). The results suggest that more miRNAs are involved in cotton anther development and response to HT stress at the TDS.

Expression of miRNAs in cotton anthers in response to HT stress

Because our focus was whether miRNAs respond to HT stress, the fold changes in the expression of miRNAs under the NT and HT treatments were calculated both within and between 84021 and H05. Twenty-seven miRNAs with $|log_2(fold changes)| > 0.8$ were chosen to create a heat map and were classified into four types (type I–IV) according to the expression pattern (Figure 2a), in which mtr-miR172a (red, type I) was the only miRNA that exhibited opposite expression changes in 84021 and H05 both at the TS and TDS. In addition, miRNAs displayed in green and purple font showed different expression patterns at only one developmental stage (TS or TDS); these miRNAs were classified as types II and III, respectively. The remaining miRNAs (black, type IV), which made up the majority, have similar

expression patterns in 84021 or H05 at both the TS and TDS, which suggests that these miRNAs may function conservatively in the response to HT stress.

To validate the reliability of the small RNA sequencing, 20 miRNAs (13 known miRNAs and seven novel miRNAs) with high or low expression levels were chosen randomly to perform real-time reverse transcriptase-polymerase chain reaction (RT-PCR). Overall, quantitative (q)RT-PCR measurements were generally in agreement with small RNA sequencing (R^2 = 0.7157; Figure 2b). According to our previous studies, auxin signal responses were implicated in male sterility under HT stress; miR156 were reported to regulate tolerance to recurring heat stress; and miR172 and its target gene *AP2* take part in development and responses to environment stresses (Wollmann *et al.*, 2010; Min *et al.*, 2014; Stief *et al.*, 2014; Nizampatnam *et al.*, 2015; Li *et al.*, 2016). Thus, the expression levels of these miRNAs of interest were detected by qRT-PCR, and the results are shown in Figure 2c–h. We found that miR156 [ahy-miR156c (ahy, *Arachis hypogaea*) and ath-miR156a-5p (ath, *Arabidopsis thaliana*) were merged together] were suppressed by HT stress in 84021 and H05 either at the TS or TDS stage (Figure 2c). However, ath-miR157a-5p was highly induced by HT stress in 84021 at the TDS stage but not in H05, and no obvious changes were found at the TS stage in 84021 and H05 (Figure 2d). The expression of ath-miR160a-5p was suppressed by HT stress in 84021 at the TS and TDS stages, but induced in H05 (Figure 2e). In addition, ath-miR167d was highly induced by HT in 84021 and H05 both at the TS and TDS stages (Figure 2f); mtr-miR172a (mtr, *Medicago truncatula*) was suppressed by HT stress in 84021 but was highly induced in H05 at the TS and TDS stages (Figure 2g); and stu-miR393-3p (stu, *Solanum tuberosum*) was induced by HT at the TS stage, but suppressed at the TDS stage (Figure 2h).

Identification of miRNA targets through degradome sequencing

As a powerful approach for the experimental identification of targets for miRNAs, degradome sequencing has been widely used for validating the cleavage sites of miRNAs (German *et al.*, 2009). Four degradome libraries (8N, 8H, HN and HH) were constructed to validate the targets of miRNAs in this study, and more than 10 million total tags were obtained. Nearly 55% of the unique tags were mapped to the TM-1 genome, and tags with annotation information are listed in Table S3. Tags annotated with cDNA_sense were then used for target prediction. As a result, a total of 347 targets (528 cleavage sites) of 76 miR-NAs were identified (Table S4).

The targets were screened under more strict conditions (category <2.5 in all samples). Following this screen, the remaining 171 targets from 22 miRNA families are listed in Table 1. More than 80% of the genes (137/171) encode TFs,
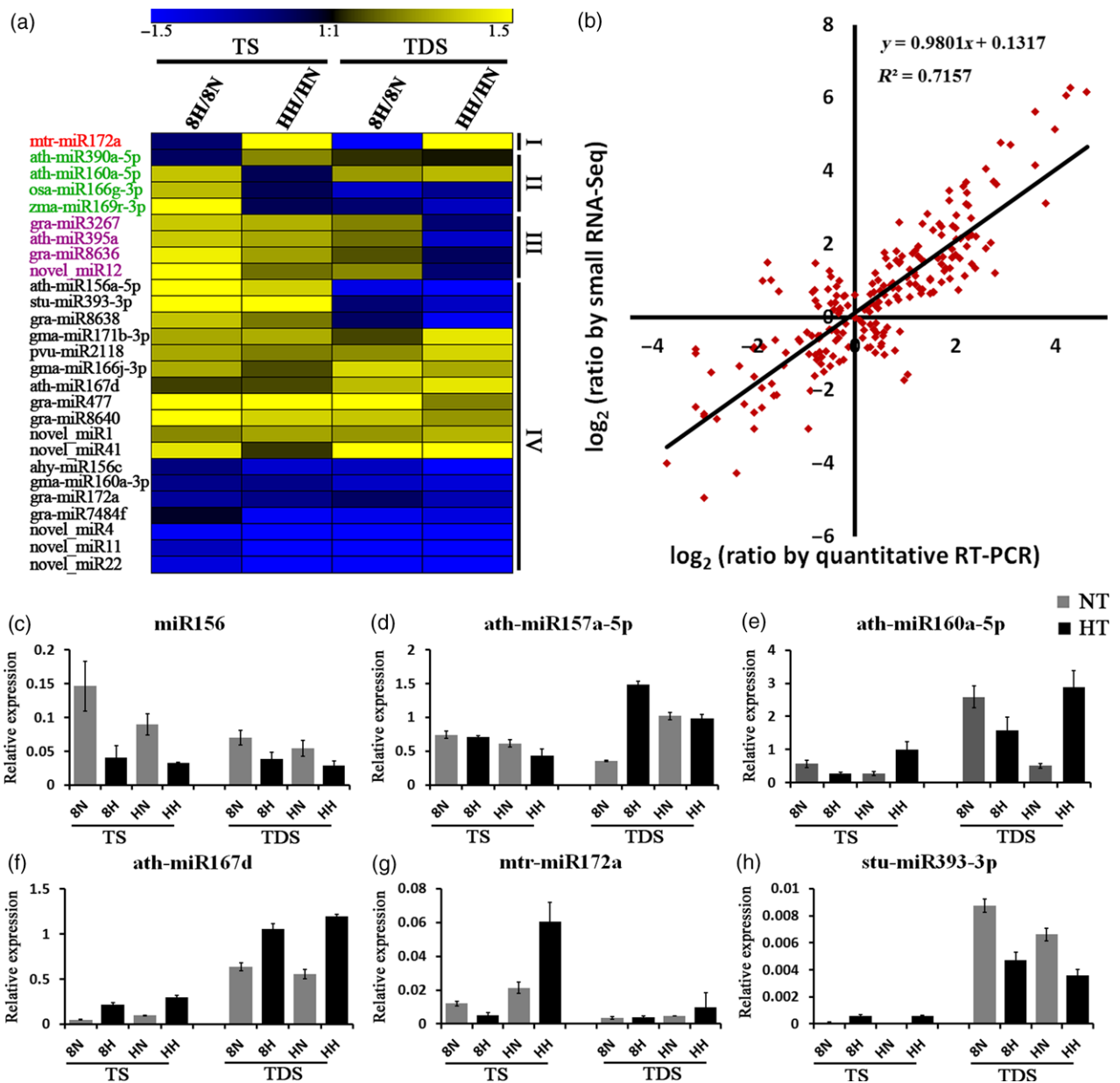
Figure 2. Heat map and quantitative reverse transcriptase-polymerase chain reaction (qRT-PCR) identification of miRNAs responding to high-temperature (HT) stress.

(a) Heat map of miRNAs responding to HT stress with |log₂ (fold changes)| >0.8. Blue and yellow colours indicate downregulated and upregulated miRNAs, respectively. miRNAs were classified into four types (I–IV) according to the expression patterns. Type I (red): expression of mtr-miR172a is the only one that exhibited opposite trends in 84021 and H05, both at the tetrad stage (TS) and the tapetal degradation stage (TDS). Type II (green): expression of miRNAs exhibited opposite trends between 84021 and H05 at the TS, but maintained the same trends at the TDS. Type III (purple): expression of miRNAs exhibited opposite trends at the TDS, but expression was upregulated at the TS. Type IV (black): expression of miRNAs exhibited the same patterns in 84021 and H05.

(b) Correlation of the miRNA expression profile between small RNA sequencing and qRT-PCR. A total of 20 randomly selected miRNAs, including 13 known miR-NAs and seven novel miRNAs, with high or low expression levels were validated by qRT-PCR in 16 samples (including two biological replicates).

(c–h) qRT-PCR analysis of miRNAs responding to HT. *GhUB7* was used as a normalization control. TS, tetrad stage; TDS, tapetum degradation stage; 8H, 84021 under HT conditions; 8N, 84021 under NT conditions; HH, H05 under HT conditions; HN, H05 under NT conditions.

including *SQUAMOSA PROMOTER BINDING PROTEIN-LIKE* (*SPL*), *APETALA 2* (*AP2*), *AUXIN RESPONSE FACTOR* (*ARF*), *AUXIN SIGNALING F-BOX* (*AFB*) class III HD-Zip, *GRAS*, *NAC* and *WRKY*. Some of these are involved in plant hormone signalling pathways, such as the *ARFs* and *AFB* involved in the auxin signalling pathway, and *GRAS* is linked to GA signal transduction. For example, *ARF10, 16* and *17* identified from our degradome sequencing data all belong to the auxin-repressed type (Vernoux *et al.*, 2011), which are the targets of ath-miR160a-5p (Figure S2). In

addition to TFs, enzymes such as UDP-glucosyltransferase (UDPG), sulphate adenylyltransferase, Dicer-like 1 and disproportionating enzyme and hydrolases were also detected by degradome sequencing (Table 1).

To verify the correction of cleavage sites obtained from degradome sequencing, six6 target genes cleaved by HT stress-related miRNAs were chosen for 5′-RNA ligase-mediated rapid amplification of cDNA ends (RLM-RACE) identification experiments (Figure 3a–f). Similar to the degradome sequencing results, the 5′-RLM-RACE results showed that the cleavage products of *SPL* (Gh_D03G0920), *ARF* (Gh_D05G0978), *HD-ZIP* (Gh_D05G1263) and *AP2* (Gh_A01G1867) were precisely mapped from the 9th to 11th position of the complementary miRNA, showing that the cleavage events occurred with miR156, miR160, miR166 and miR172. However, Gh_A12G0866 (*SPL*) was cleaved not only by ahy-miR156c at the 706 site but also by ath-miR156a-5p and ptc-miR156k (ptc, *Populus trichocarpa*) at the 705 site (Table S4), which means that some target genes can be regulated by different miRNAs at the post-transcriptional level.

Because Since miRNAs usually work through cleaving their targets, the expression levels of targets would be expected to be negatively correlated with expression levels of their corresponding miRNAs. To assess the influence of the miRNAs on their targets, the expression of miRNA targets was examined by qRT-PCR, and the nine noteworthy miRNA/target correlation modules are shown in Figure 3g–o. Most target genes exhibited the opposite expression trend with their corresponding miRNAs (TPM from small RNA sequencing). In previous reports, various TFs, such as SPLs, ARFs and AP2, have been found to be involved in anther development (Wu *et al.*, 2006; Wollmann *et al.*, 2010; Xing *et al.*, 2010; Shi *et al.*, 2015); these TFs are the targets of multiple miRNA families. In the present study, the *SPLs* were induced by HT stress in most cases, with the exception of Gh_A03G1092, which was upregulated in 84021 but downregulated in H05 at the TS. In addition, *ARFs* were highly induced by HT stress at the TS, but were suppressed at the TDS in both 84021 and H05. *AP2*, the target of miR172, was suppressed at the TS but induced at the TDS in H05, but *AP2* did not show obvious changes in 84021. *UDPG* is identified as a new target of miR167 and was suppressed by HT stress.

In summary, 5′-RLM-RACE confirmed that the target genes validated from degradome sequencing were correctly cleaved by the corresponding miRNAs, and the expression trend of target genes exhibited an opposite relationship with the miRNA abundance in the anthers.

Overexpressing miR160 leads to anther indehiscence under HT stress

Auxin signalling has been proven to be involved in male sterility under HT conditions (Min *et al.*, 2014), but the detailed molecular mechanism still remains unclear. In this research, *ARF10*, *16* and *17*, three auxin-repressed *ARFs*, were identified as the target genes of miR160 and strongly responded to HT stress. To identify the function of miR160 in the cotton anther response to HT stress, a miR160 overexpression cotton line (miR160 OE2) was obtained, which showed high miRNA160 expression in TS and TDS anthers under NT condition (Figure 4a). Correspondingly, the expression of both target genes (*ARF10* and *ARF17*) was suppressed in overexpression line (Figure 4a). Under NT conditions, the anther of the miR160 transgenic cotton line was fertile like its null control (Figure 4b). After HT treatment for 5 days, the miR160 transgenic cotton line showed anther indehiscence, but with viable pollen grains. The null control showed normal anther fertility (Figure 4b). The anthers of miR160 OE2 and null control both showed anther indehiscence and partial pollen abortion after HT stress treatment for 7 days, with the phenotypes looking like the H05 after HT stress treatment for 7 days – the transgenic host line (YZ1) is also sensitive to HT stress.

ARF17 was reported responsible for primexine formation and pollen development through regulating the expression of *CALLOSE SYNTHASE5* (*Cals5*), the major gene for callose biosynthesis (Yang *et al.*, 2013). In our study, expression of *ARF17* (*Gh_A05G1991*) was suppressed in miR160 OE line (Figure 4a), indicating overexpression of miR160 had effects on callose synthesis and pollen wall formation. Meanwhile the expression of *Cals5* and the accumulation of callose was detected in anthers from miR160 OE line and null control at TS stage (Figure S3), the result showed that the expression of *Cals5* and the accumulation of callose both had no obvious changes between miR160 OE line and null control under NT or HT conditions alone (Figure S3), corresponding to the fertility pollen grains in anthers of miR160 OE line under HT stress for 5 days (Figure 4b). However, the fluorescent signal of aniline blue staining in callose was stronger under HT than under NT, which might be responsible for the pollen grains abortion in anthers of miR160 OE line and null control after HT treatment for 7 days (Figure 4b).

It has been reported that some mutants in *Arabidopsis*, such as *non-dehiscence 1*, *delayed-dehiscence 1* (*dde1*) and *delayed-dehiscence 2* (*dde2*), display anther indehiscence but contain viable pollen grains (Sanders *et al.*, 1999), similar to the phenotype of our miR160 OE line (HT treatment for 5 days). The *dde1* mutant is a loss function of *OXOPHYTODIENOATE-REDUCTASE 3* (*OPR*), a JA biosynthetic enzyme gene, and mutants of JA biosynthetic genes always result in anther indehiscence (Sanders *et al.*, 2000). In addition, it has been reported that auxin receptor mutants promote JA biosynthesis in Arabidopsis, suggesting that auxin negatively regulates JA content in rice anther dehiscence (Cecchetti *et al.*, 2013; Zhao *et al.*, 2013). We therefore measured the expression levels of JA

Table 1 miRNA targets assembly with category <2.5

miRNA_family (22)	Annotation	Number of targets (171)	Degradome category	Targets gene ID [*G. hirsutum* TM-1 (AD)1]
miR156/157	Squamosa promoter binding protein-like 15	1	0	Gh_A11G2811
	Squamosa promoter binding protein-like 2	6	0	Gh_A03G1092, Gh_A04G1486, Gh_D04G1827, Gh_D02G1515, Gh_A01G1281, Gh_D01G1503
	Squamosa promoter binding protein-like 10	4	1	Gh_D12G0947, Gh_A12G0866, Gh_A11G0706, Gh_D11G0821
	Protein phosphatase 2A, regulatory subunit PR55	1	1.5	Gh_A06G0796
	Squamosa promoter-binding protein-like (SBP domain) transcription factor family protein	9	0.5–1	Gh_A13G0749,Gh_A01G1274, Gh_A11G0344, Gh_A03G1083, Gh_D02G1499, Gh_D01G1495, Gh_A12G1380, Gh_D12G1504, Gh_D11G0401
	Squamosa promoter binding like protein 6-like (*Vitis vinifera*)	2	0.5–1	Gh_D13G0874, Gh_D03G0920
	Squamosa promoter binding protein-like 9	4	0–1	Gh_A04G1331, Gh_D04G1985, Gh_D11G3165, Gh_A01G2095
miR160	Auxin response factor 17	4	0.5	Gh_A06G0332, Gh_A05G1991, Gh_D05G3805, Gh_D06G0360
	Auxin response factor 10	4	1	Gh_A03G0274, Gh_D05G0978, Gh_A05G0895, Gh_D03G1293
	Auxin response factor 16	8	0.5–2	Gh_A05G3576, Gh_A10G1836, Gh_D04G0030, Gh_D09G1405, Gh_A09G1401, Gh_D10G2093, Gh_A13G2013, Gh_D13G2411
miR162	Dicer-like 1	2	1	Gh_A07G1222, Gh_D07G1326
miR164	NAC (No Apical Meristem) domain transcriptional regulator superfamily protein	1	2	Gh_A11G2580
miR166	Homeobox-leucine zipper family protein/lipid-binding START domain-containing protein	12	1.5	Gh_D08G2109, Gh_A13G2011, Gh_A08G1765, Gh_D10G0038, Gh_D03G1290, Gh_A10G0035, Gh_D13G2409, Gh_D05G0975, Gh_A05G0892, Gh_A03G0276, Gh_D05G1263, Gh_A05G1085
	Class III HD-Zip protein 8 (*Populus trichocarpa*)	5	2.5	Gh_A13G1004, Gh_A06G0833, Gh_D06G0966, Gh_D05G0479, Gh_A06G0741
miR167	UDP-glucosyltransferase, putative (*Ricinus communis*)	1	2.5	Gh_D12G0458
	Cytochrome P450 71A1-like (*Fragaria vesca subsp. vesca*)	2	2.5	Gh_A13G0215, Gh_A13G0217
miR168	Eukaryotic translation initiation factor 2c, putative (*Ricinus communis*)	4	2	Gh_A12G2469, Gh_D12G2597, Gh_D09G1629, Gh_A09G1557
miR171	GRAS family transcription factor	8	0.5	Gh_A03G0093, Gh_D12G2185, Gh_A12G2009, Gh_D03G1558, Gh_D12G0935, Gh_A12G0855, Gh_D12G0934, Gh_A12G0854
miR172	Predicted: ethylene-responsive transcription factor RAP2-7-like (*Vitis vinifera*)	5	0–1.5	Gh_D03G1282, Gh_A03G0292, Gh_A05G0861 Gh_D05G3873, Gh_D08G0014
	Floral homeotic protein APETALA 2, putative (*Ricinus communis*)	2	1	Gh_D01G2112, Gh_A01G1867
	Protein of unknown function (DUF668)	3	2.5	Gh_A05G3411, Gh_D04G0180, Gh_D04G0178
	Transcription factor APETALA2 (*Vitis vinifera*)	7	2–2.5	Gh_D12G0675, Gh_A02G1495, Gh_A11G1795, Gh_D03G0218, Gh_D11G1956, Gh_A10G0822, Gh_A12G0670

Table 1. (continued)

miRNA_family (22)	Annotation	Number of targets (171)	Degradome category	Targets gene ID [*G. hirsutum* TM-1 (AD)1]
miR393	F-box/RNI-like superfamily protein	6	1	Gh_D08G0763, Gh_A08G0662, Gh_A08G1014, Gh_D11G1228, Gh_A08G0390, Gh_D08G1288
	Auxin signalling F-box 2	4	2	Gh_D07G2334, Gh_A07G2125, Gh_D11G0671, Gh_A11G0586
miR395	Sulphate adenylyltransferase, putative (*Ricinus communis*)	2	2.5	Gh_A09G1922, Gh_D09G2130
	Unknown function	1	2.5	Gh_A02G0101
miR396	Growth-regulating factor 1	8	2	Gh_A06G0219, Gh_A05G1848, Gh_A10G0804, Gh_D05G2044, Gh_A02G0827, Gh_D10G0959, Gh_D03G0282, Gh_A02G1438
	Growth-regulating factor 2	1	2	Gh_D11G0870
	Growth-regulating factor 3	1	2	Gh_D09G1332
	Growth-regulating factor 5	3	2	Gh_A13G1692, Gh_A10G0492, Gh_D13G2042
	Growth-regulating factor 7	1	2	Gh_D12G2699
	Growth-regulating factor 8	2	2	Gh_D12G2356, Gh_A12G2177
	Growth-regulating factor 9	7	2–2.5	Gh_A13G1365, Gh_A11G0749, Gh_D12G2219, Gh_D13G1673, Gh_A12G2042, Gh_A02G1205, Gh_D03G0527
	DENN (AEX-3) domain-containing protein	1	2	Gh_D05G0338
	Unknown function	1	2.5	Gh_D07G0378
miR397	Laccase/diphenol oxidase family protein	2	1–1.5	Gh_A05G0758, Gh_D05G0888
	Proton gradient regulation 3	6	1–2.5	Gh_A04G0297, Gh_D05G3362, Gh_A04G0293, Gh_A04G0308, Gh_D05G3346, Gh_A10G1155
	Pentatricopeptide repeat (PPR) superfamily protein	5	1	Gh_A04G0298, Gh_D05G3389, Gh_D05G3391, Gh_A10G1190, Gh_A07G1073
	Tetratricopeptide repeat (TPR)-like superfamily protein	2	1	Gh_A04G0299, Gh_D09G0552
	Nuclear transport factor 2 (NTF2) family protein with RNA binding domain	1	2.5	Gh_A07G1426
miR858	GHMYB38 (*Gossypium hirsutum*)	1	2.5	Gh_Sca005689G01
	GHMYB36 (*Gossypium hirsutum*)	1	2.5	Gh_D07G0168
	GHMYB10 (*Gossypium hirsutum*)	1	2.5	Gh_A06G0676
miR2275	Unknown function	1	2.5	Gh_D05G1695
miR2947	Hydrolases;protein serine/threonine phosphatases	1	2	Gh_D01G1409
miR3954	NAC 014	2	2.5	Gh_D02G0122, Gh_D02G0123
miR7492	Disproportionating enzyme 2	1	2.5	Gh_A06G0991
miR7505	Pentatricopeptide repeat (PPR-like) superfamily protein	3	1–2.5	Gh_D05G3380, Gh_A04G1307, Gh_D10G1342
miR8746	Disease resistance protein (TIR-NBS-LRR class)	2	0.5	Gh_A03G0215, Gh_D03G1355
novel_mir_1	Unknown function	1	2	Gh_A11G2859
novel_mir_9	ATP binding valine-tRNA ligases; aminoacyl-tRNA ligases; nucleotide binding;	1	0	Gh_A08G2278
	peroxin 5	1	0	Gh_A13G2067
novel_mir_16	Protein of unknown function (DUF567)	1	2.5	Gh_A08G2356
novel_mir_18	Unknown function	3	0	Gh_D11G3234, Gh_A06G0841, Gh_D06G0974
	FRAGILE HISTIDINE TRIAD	1	2.5	Gh_A10G1050
novel_mir_171	TATA binding protein 2	1	1	Gh_A11G2339

Function annotation of target genes comes from NCBI GenBank and Tair 10.

biosynthesis-related genes, including *DEFECTIVE ANTHER DEHISCENCE 1* (*DAD1*), *DDE2*, *OPR3* and *LIPOXYGENASE 4* (*LOX4*), in the miR160 OE line and its null control under NT and HT for 7 days (Figure S4). *DDE2* has no obvious difference in expression between miR160 OE line and the null control, but is highly induced by HT stress. The
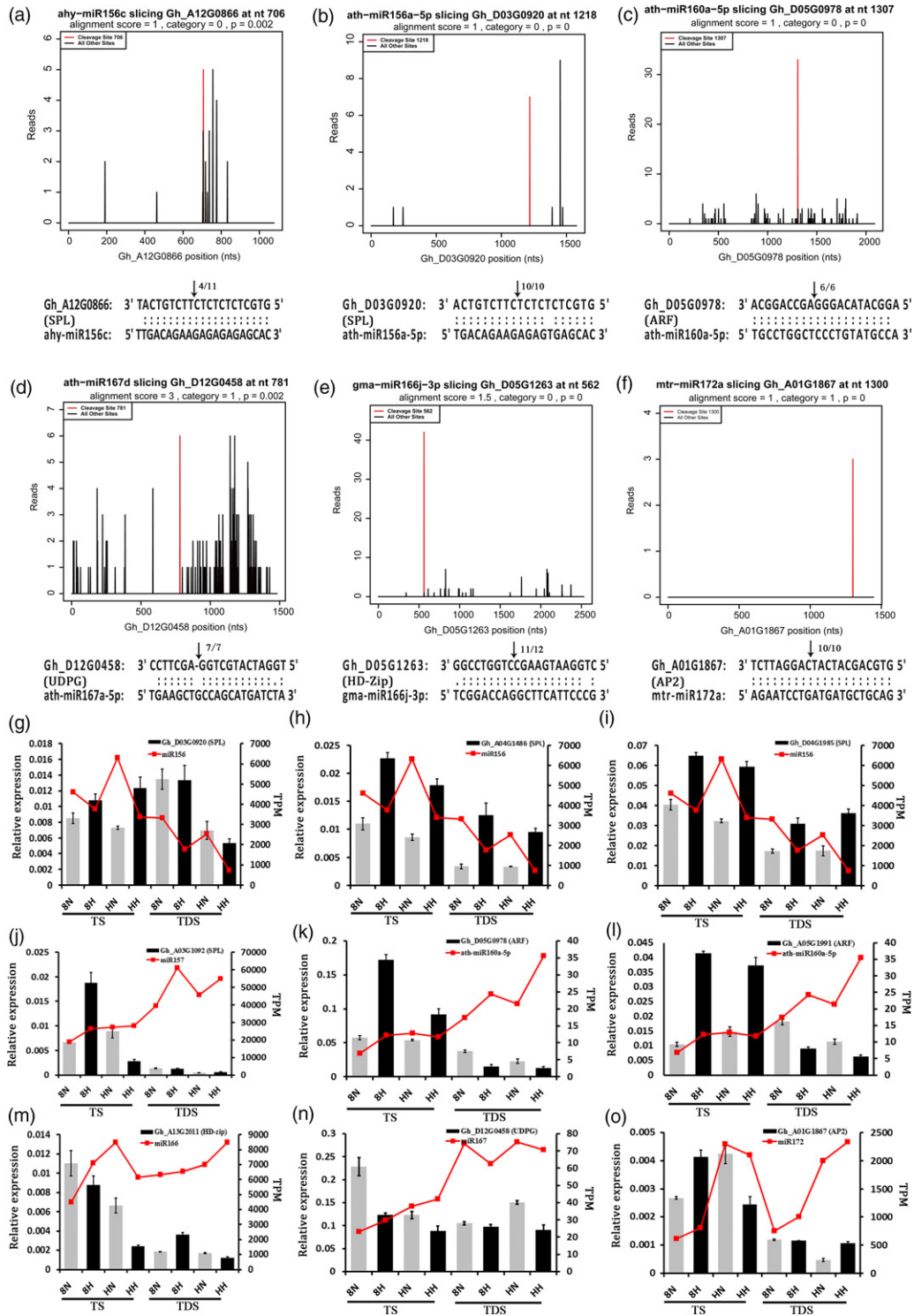
Figure 3. Target plots (T-plots) and expression levels of miRNA targets.

(a–f) T-plots of miRNA targets. Arrows indicate the cleavage sites for miRNAs, and the ratio indicates the corrected cleavage events validated through RNA ligase-mediated rapid amplification of cDNA ends (RLM-RACE).

(g–o) The relative expression levels of miRNA targets at the tetrad stage (TS) and tapetal degradation stage (TDS). The histogram and line indicate the expression levels of targets [quantitative reverse transcriptase-polymerase chain reaction (qRT-PCR) results] and miRNA [transcripts per million (TPM) from sequencing], respectively.

TS, tetrad stage; TDS, tapetum degradation stage; 8H, 84021 under high-temperature (HT) conditions; 8N, 84021 under normal-temperature (NT) conditions; HH, H05 under HT conditions; HN, H05 under NT conditions.
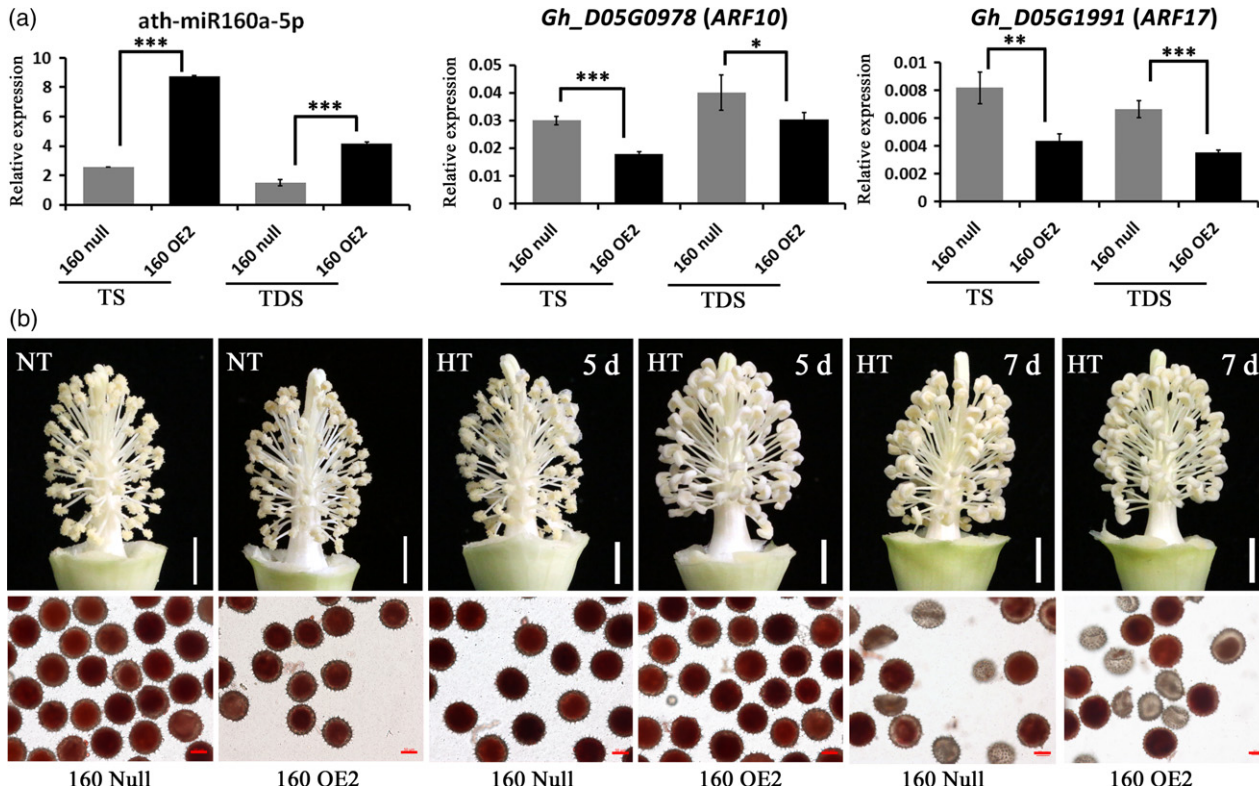
(a)

(b)

Figure 4. Overexpression of miR160 increased anther sensitive to high-temperature (HT) stress in cotton.
(a) The expression changes of ath-miR160a-5p ant its target genes *ARF10* and *ARF17* in the transgenic cotton anthers at the tetrad stage (TS) and tapetal degradation stage (TDS) under normal-temperature (NT) conditions. *GhUB7* was used as the control. Asterisks indicate statistically significant differences (*$P < 0.05$, **$P < 0.01$, ***$P < 0.001$) by Student's *t*-test.
(b) The phenotype of anther and pollen activity of control and miR160 overexpression lines under NT and HT conditions. Anthers of miR160 OE and control plants can dehisce normally with fertile pollen grains under NT conditions. However, the miR160 overexpression line showed indehiscent anthers but fertile pollen grains after HT treatment for 5 days, and the anther fertility of null control is normal. After HT treatment for 7 days, anthers of miR160 and null control all showed male sterility with indehiscence anther and partly pollen abortion. Tetrazolium chloride (TTC) was used for staining of pollen grains. Scale bars: 5 mm (white); 50 μm (red).

expression of *DAD1*, *OPR3* and *LOX4* was induced by HT stress, but with much lower expression levels in the miR160 OE line than in the null control, which indicates that JA biosynthesis is suppressed in anthers of the miR160 OE line relative to its null control under HT stress. We conclude that overexpression of miR160 suppresses the expression level of auxin-repressed-type *ARFs* (*ARF10, 17*), which causes activation of auxin signalling and suppresses JA biosynthesis, and ultimately leads to anther indehiscence under HT stress.

Activation of auxin signalling leads to male sterility in cotton under HT stress

To verify the active auxin signalling function in cotton male sterility under HT stress, IAA application experiments were performed with 84021 and H05 anthers under NT and HT conditions (Figure 5). The results show that 84021 remained completely fertile (Figure 5a, e and i) when treated only with HT and that H05 showed complete anther indehiscence, with pollen grains partially inactive

Figure 5. Phenotyping of anther dehiscence and pollen fertility and gene expression analysis of cultivars 84021 and H05 under indole-3-acetic acid (IAA) and high-temperature (HT) treatments.
(a–d) Degrees of anther dehiscence and pollen fertility of 84021 and H05 under IAA and HT treatments. The anthers of 84021 can undergo dehiscence normally under HT stress, but undergo partial indehiscence with IAA treatment. The anthers of H05 are much more sensitive than those of 84021, which is almost indehiscent under HT and becomes completely indehiscent with IAA treatment. Scale bar: 5 mm.
(e–h) Enlarged views of (a–d).
(i–l) Tetrazolium chloride (TTC) staining of pollen grains. Pollen activity of 84021 is normal under HT stress, but pollen activity is partially sterile under HT and IAA treatments; H05 as an HT-sensitive cultivar showed partial sterility under HT stress and complete sterility when IAA was applied under the HT treatment. Red arrows represent sterile anthers or pollen; white and black arrows refer to fertile anthers or pollen, respectively. Scale bar: 50 μm.
(m–p) The relative expression levels of miR160, *YUC2*, *ARF10* and *ARF17* were identified by quantitative reverse transcriptase-polymerase chain reaction (qRT-PCR) in anthers at the tetrad stage (TS) and the tapetal degradation stage (TDS). *GhUB7* was used as the control. Values with different letters are considered statistically significant (shortest significant range; $P < 0.05$).

84021 HT Mock	H05 HT Mock	84021 HT + IAA Treat	H05 HT + IAA Treat
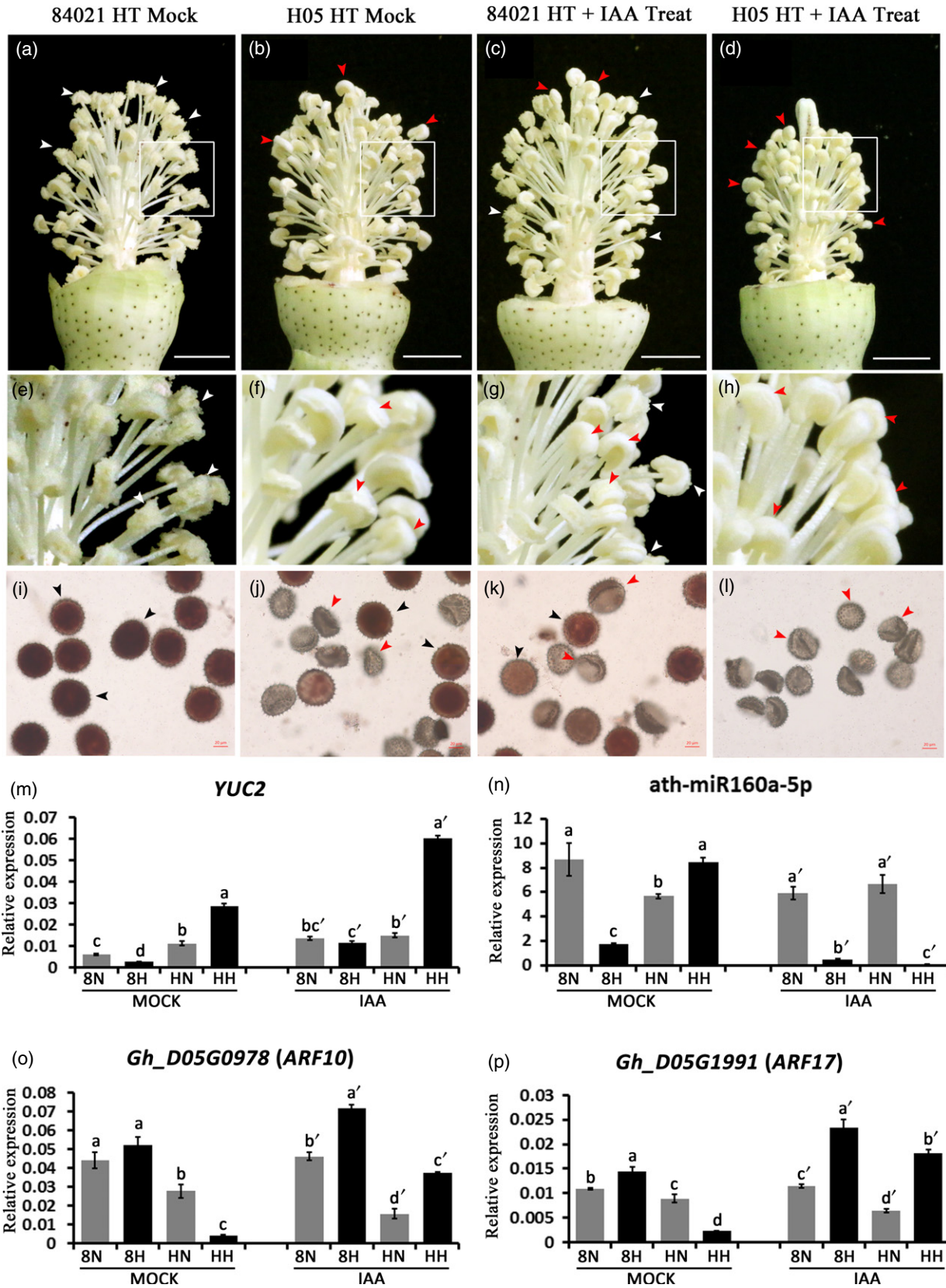
(Figure 5b, f and j). Once the anthers were treated with exogenous IAA under HT conditions, 84021 displayed male sterility by exhibiting indehiscent anthers and inactive pollen grains to some degree (Figure 5c, g and k), while H05 showed more serious male sterility, with much shorter filaments, more pinched anthers and completely inactive pollen grains, compared with HT treatment alone (Figure 5d, h and l). These results imply that activation of auxin signalling is harmful to cotton anther development under HT stress, adversely affecting microspore development and anther dehiscence.

The expression levels of miR160, *YUC2*, *ARF10* and *ARF17* were monitored at the TDS stage. Results show that *YUC2* was highly induced in H05 by HT stress with or without IAA treatment, but no obvious expression changes were found in 84021 (Figure 5m). In addition, miR160 was suppressed by HT stress in 84021 but highly induced in H05 without IAA treatment (Figure 5n, Mock), and the expression was extremely suppressed by HT stress after IAA application both in 84021 and H05 (Figure 5n, IAA). Correspondingly, the expression levels of *ARF10* and *ARF17* increased in 84021 after HT stress and decreased in H05 without IAA treatment (Figure 5o and p, Mock), but were induced by HT stress after IAA application (Figure 5o and p, IAA). The above analysis of miR160 and gene expression changes after HT and IAA treatment suggest that auxin signalling is activated by HT in H05, which leads to male sterility under HT stress. However, once exogenous IAA was applied to the anthers under HT conditions, the expression of miR160 was strongly suppressed, preventing the activation of auxin signalling to maintain anther fertility.

Overexpression of miR157 induces sensitivity of cotton anthers to HT stress

In our small RNA sequencing data, the miR156/157 family is the most abundant miRNA family and contains three members: ahy-miR156c, ath-miR156a-5p and ath-miR157a-5p, all of which exhibit a strong response to HT stress. In our recent work, overexpression of miR157 suppressed the auxin signal in cotton ovules and young buds (<2 mm; Liu *et al.*, 2017). Thus, two lines of miR157 overexpression plants were used to identify the potential function of the miR156/157 family in the response of cotton anthers to HT stress. Because the organs of transgenic lines are smaller than those of the controls (Figure S5a–c), we first rebuilt the relationship between bud length and anther developmental stage (Figure S5d–l) according to the earlier research (Wu *et al.*, 2015). The results show that the anther developmental stages of 5–6 mm (TS) and 7–12 mm (TDS) buds from miR157 transgenic plants corresponded to the 6–7 mm (TS) and 9–14 mm (TDS) buds from wild-type plants, respectively. Although the floral organ size of the two miR157 overexpression lines was smaller and the number of anthers was much less than those of the control

(Figure 6a), the transgenic plants still could produce fertile pollen grains under NT conditions (Figure 6c–e). After HT treatment, the stamens of plants overexpressing miR157 were more sensitive to HT stress, producing indehiscent anthers and sterile pollen grains (Figure 6b, f–h).

Gene expression analysis showed that the miR157 was induced by HT stress, and much higher expression levels were detected in transgenic lines under NT and HT conditions at the TS and TDS (Figure 6i). Accordingly, *SPLs* had lower expression levels in transgenic plants than in controls, although *SPLs* could be induced by HT, except for *SPL6* at the TS (Figure 6j and k). In addition, *YUC5* as an auxin biosynthesis gene was induced by HT stress at the TDS but was suppressed in plants overexpressing miR157 compared with the controls (Figure 6l). These results show that overexpressing miR157 first affects the differentiation of anther primordia, resulting in fewer numbers of anthers. The auxin signal is then extremely suppressed in the anthers of miR157 overexpression lines, which leads to anther indehiscence and microspore abortion under HT conditions.

Various miRNAs and their target genes generate cotton male sterility under HT stress

The simplified schematic in Figure 7 shows how the miRNAs and genes are involved in generating male sterility under HT stress in cotton. We propose that HT stress induces the expression of miR160 in H05, which then suppresses the expression of auxin-repressed-type *ARFs* (*ARF10*, *17*) and causes the activation of auxin signalling, ultimately leading to anther indehiscence. On the other hand, the expression of miR156/157 is suppressed by HT stress in H05 and 84021 (Figure 2), and overexpression of miR157 suppresses the biosynthesis of auxin (Figure 6); therefore, HT stress appears to activate the auxin signalling pathway by suppressing the expression of miR156/157.

DISCUSSION

Male sterility caused by long-term HT stress has been observed and utilized for breeding for many years, but the molecular mechanism remains unclear. Epigenetic modification is believed to be an important way by which plants respond to HT stress, contributing to TGMS formation. miRNAs are a class of non-coding RNAs that play a key role in epigenetic modification, and we investigated whether they might be involved in male sterility in plant responses to HT stress.

Small RNAs are involved in anther development and respond to HT stress

Our results show several interesting phenomena regarding the distribution and expression changes of small RNAs. First, the percentage of small RNA reads that mapped to the genome decreased with anther development but increased after HT treatment, which has not been reported
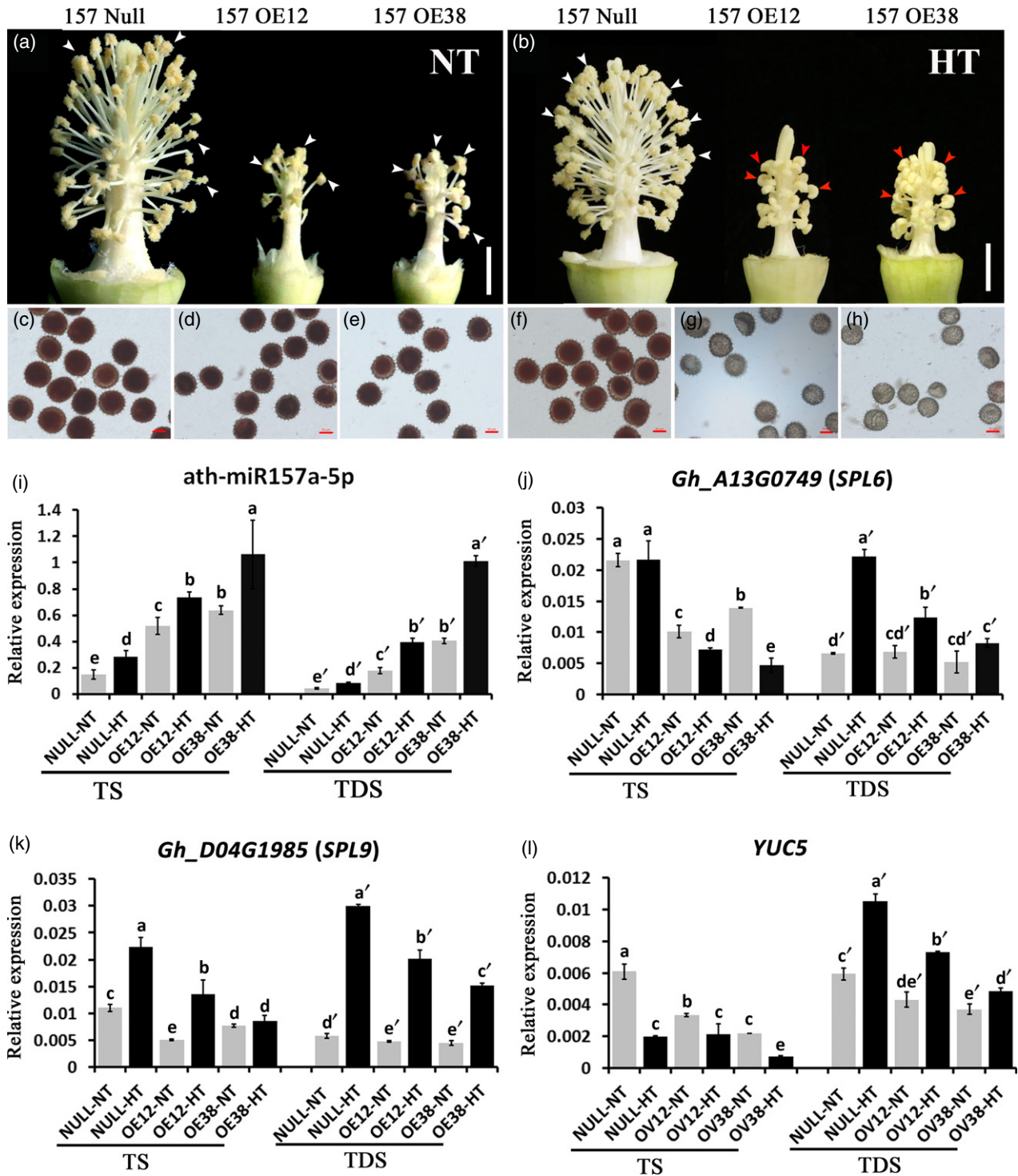
Figure 6. miR157 overexpression cotton lines show more sensitivity to high-temperature (HT) stress.

(a) Anthers of miR157 overexpression lines and the control dehisce normally under normal-temperature (NT) conditions.

(b) Anthers of control plants remain completely fertile but are indehiscent in miR157 overexpression lines under HT.

(c–e) Pollen grains are completely fertile in miR157 overexpression lines and controls under NT conditions.

(f–h) Pollen grains are completely fertile in control plants but abortive in transgenic lines under HT.

(i–l) The relative expression levels of miR157, *SPL6*, *SPL9* and *YUC5* were identified by quantitative reverse transcriptase-polymerase chain reaction (qRT-PCR) in anthers at the tetrad stage (TS) and the tapetal degradation stage (TDS). Values with different letters are considered statistically significant (shortest significant range; $P < 0.05$).

Scale bars: 5 mm (white); 50 μm (red). White arrows represent normal anther dehiscence; red arrows indicate anther indehiscence. *GhUB7* was used as the control.
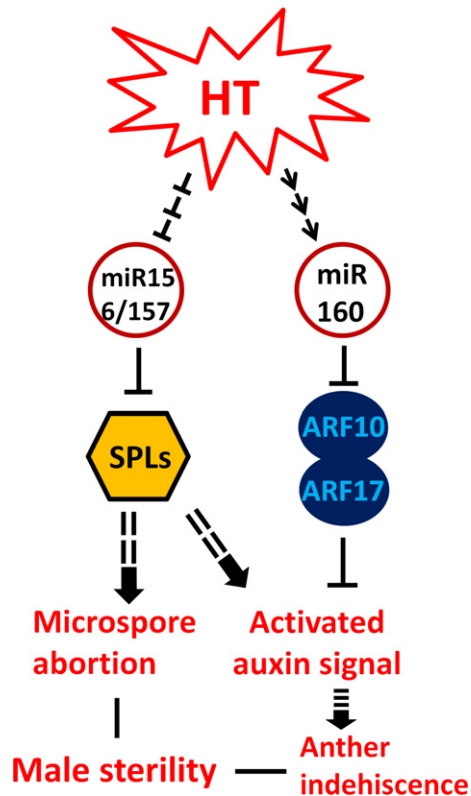
Figure 7. A schematic showing various miRNAs involved in cotton male sterility caused by high-temperature (HT) stress.

The expression level of miR156/157 can be suppressed by HT, which, as a result, changes the expression level of SPLs, leading to a disordered floral organ development process and ultimately causing male sterility through unknown pathways. At the same time, the auxin signal can be excessively activated by HT stress through suppressing the expression of miR160 and influencing the transcription level of their target ARFs. The activated auxin signalling can lead to anther indehiscence, which ultimately results in male sterility under HT conditions through unknown pathways. [Colour figure can be viewed at wileyonlinelibrary.com].

the TDS may indicate that stronger post-transcriptional regulation occurred, which might involve the process of microspore genesis and PCD of the tapetum. These results show that small RNAs play an important role in anther development and in the response to long-term HT stress, although the exact mechanism remains unknown.

Auxin signalling modulation in anthers is essential to male fertility in cotton

In cotton, it has been proven from our results and from those of other reports that exogenous IAA treatment leads to male sterility under long-term HT stress (Yasuor *et al.*, 2006; Min *et al.*, 2014). In addition, endogenous IAA levels have been reported to increase at the TDS in the HT-sensitive cultivar H05 (Min *et al.*, 2014). In this study, overexpression of miR160 led to activation of auxin signalling and ultimately resulted in anther indehiscence. Reports from Arabidopsis showed that anther dehiscence occurs earlier in auxin perception mutants (*afb1-3* and *tir1afb2af-b3*) due to enhanced JA biosynthesis (Cecchetti *et al.*, 2013). The JA signal was proven earlier to be necessary for anther dehiscence (Devoto *et al.*, 2002), which indicates that excessive auxin signalling might lead to anther indehiscence through suppressing JA biosynthesis.

However, endogenous auxin levels of anthers in barley and *Arabidopsis* significantly decreased under HT conditions, and exogenous auxin could completely reverse male sterility caused by HT stress (Sakata *et al.*, 2010). Auxin was proven necessary for floral development in an earlier study, as the *YUCCA* double and triple mutants always lost male fertility (Cheng *et al.*, 2006). Interestingly, suppressed auxin signalling in cotton plants overexpressing miR157 also results in male sterility under HT stress. These results indicate that higher or lower levels of auxin are both detrimental to male fertility. Thus, a tightly regulated auxin signalling pathway must be essential for anther development under HT stress.

miRNAs are involved in the anther response to HT stress in cotton

Research in Arabidopsis showed that miR156 enhances the heat stress memory by regulating its targets of *SPLs* (Stief *et al.*, 2014). However, in our research a cotton line overexpressing miR157 showed more male sterility under HT stress (Figure 5). It has been reported that *SPLs* are essential for anther development, and loss of SPL function always leads to male sterility in many plants (Xing *et al.*, 2010, 2013; Ye *et al.*, 2010; Wang *et al.*, 2016), which might explain why male sterility occurred in cotton lines overexpressing miR157 under HT conditions. In a recent report, the transcription of miR156 was activated by auxin in the lateral roots of Arabidopsis (Yu *et al.*, 2015). However, in miR157 overexpression cotton lines, the auxin signal was suppressed in ovules and young cotton buds (<2 mm; Liu

previously. Second, the ratio of 24/21 nt small RNAs decreased from the TS to the TDS but increased after HT stress, except in 84021 at the TS. Third, reads of miRNAs at the TDS are nearly twofold higher than those at the TS. These results indicate that potential epigenetic changes occur during anther development under HT conditions. The higher number of reads mapping to the genome after HT stress indicates that a series of new small RNAs may be generated. In previous studies, DNA methylation was found to increase from the TS to the TDS, but DNA methylation decreased with HT treatment, except in 84021 at the TS (Min *et al.*, 2014), which corresponds to the small RNA mapping results but not to the 24/21 nt ratio changes. It has been reported that 24 nt small interfering RNAs (siRNAs) are important for RNA-directed DNA methylation (Matzke and Mosher, 2014). However, it is unclear why higher levels of 24 nt small RNA are in parallel with lower DNA methylation levels at the TS. More miRNA reads at

et al., 2017), which is consistent with our present research. Thus, the relationship between miR156 and auxin signalling still remains unclear and needs more studies to dissect the connections in detail.

We show that miR160 is a key repressor of auxin-repressed-type ARFs, which could be highly suppressed in 84021 at the TS and TDS (Figure 2). In addition, the overexpression of miR160 in cotton leads to anther indehiscence under HT conditions (Figure 4), possibly due to the excessive activation of auxin signalling. In previous studies, ARF17 was found to be essential for pollen wall formation (Shi *et al.*, 2015). However, no phenotypic defects were found for *arf10* or *arf16* single mutants in Arabidopsis (Okushima *et al.*, 2005), and the *arf10 arf16* double mutant showed the absence of lateral roots, which are caused by a strong auxin signal (Wang *et al.*, 2005).

In addition to miR160, miR167 is another miRNA that can regulate *ARF6* and *ARF8*, the auxin-activated-type ARFs, responsible for auxin signal transduction (Wu *et al.*, 2006). In our degradome sequencing data, UDPG was identified as another target of miR167 (Figure 3), which suggests that auxin and sugar signals might be concurrently regulated by miR167. miR167 was induced by HT stress, which might cause a change of auxin signalling by miR167 by regulating target ARFs or UDPG.

From the sequencing results, 27 miRNAs were identified as responding to HT stress (Figure 2b). Of these, miR172 is the only miRNA to show a different expression pattern between 84021 and H05 both at the TS and TDS; the target gene of miR172 is the AP2 class of TFs. From our degradome sequencing data, the major two types of AP2 (RAP2.7 and AP2) were identified. AP2, a key factor during the differentiation of floral organs, is necessary for anther formation and development (Huang *et al.*, 2016). RAP2.7 (also known as TARGET OF EAT1, TOE1) was reported to interact with a subset of JAZ proteins and repress the transcription of *FLOWERING LOCUS T*, resulting in delayed flowering time in Arabidopsis (Zhai *et al.*, 2015). It is therefore possible that HT stress affects anther development by regulating the expression of miR172.

In summary, various miRNAs were found involved in cotton anther response to HT stress. Activation of auxin signalling is proposed to be an important reason for male sterility in H05 under HT conditions, and miR160 was identified as a component of this process. miR156/157 was also found to be a component of the auxin signalling pathway, influencing anther development via regulation of *SPLs*.

EXPERIMENTAL PROCEDURES

Plant materials and growth conditions

The cotton (*G. hirsutum*) cultivars used in this research included 84021 (HT-insensitive line), H05 (HT-sensitive line), miR157 and miR160 overexpression transgenic cotton lines and a control, as described in our previous study (Liu *et al.*, 2014). Cotton seeds were sown and grown in greenhouses with a 12/12 h photoperiod and a 28–35°C/20–28°C day/night thermoperiod until flowering (normal conditions). To identify the growth progress of cotton buds under normal conditions, the bud length was recorded every day until flowering by measuring the length from the nectary to the top of the bud with a Vernier calliper. For the HT treatment, temperature conditions were reset to a 39 $\pm$ 2°C/29 $\pm$ 2°C day/night thermoperiod and lasted for nearly 7 days. When the anthers of H05 showed male sterility, the flower buds of all sizes were harvested from the HT and NT conditions and classified into different development stages according to previous studies (Wu *et al.*, 2015). The sampled anthers were frozen in liquid nitrogen for later use.

Small RNA and degradome library construction

Sixteen samples were used for small RNA sequencing that contained two developmental stages, the TS and TDS; two temperature conditions, HT and NT; two cultivars, 84021 and H05; and two biological replicates.

Total RNA was extracted according to the modified guidelines for the thiocyanate protocol (Zhu *et al.*, 2005). To ensure the quality of RNA for library construction, all total RNA samples were sent to the Beijing Genomics Institute (BGI) for quality testing using an Agilent 2100 Bioanalyzer system. Briefly, small RNAs (~18–30 nt) were separated from the total RNA using a polyacrylamide gel electrophoresis gel, and then were purified and ligated with 3″ and 5″ adapters. To obtain sufficient fragments for Illumina sequencing, a reverse transcription reaction was then performed to generate cDNA, which was used for subsequent PCR amplification. PCR products were purified and dissolved in elution buffer solution, and tested again with the 2100 Bioanalyzer system before Illumina sequencing.

Four degradome libraries (8N, 8H, HN and HH) were constructed as previously described (8N, 84021 under NT; 8H, 84021 under HT; HN, H05 under NT; and HH, H05 under HT; Addo-Quaye *et al.*, 2008). Degradome libraries were constructed with mixed samples, ignoring the differences in developmental stage. In brief, mRNA fragments with poly (A$^+$) sequences were annealed and captured with a streptavidin system and magnetic beads using biotinylated random primers. 5′ RNA adapters were ligated to RNAs containing 5′-monophosphates. Purified ligated products were reverse-transcribed to cDNA and then amplified with PCR. PCR products were digested with *Mmel* and ligated with a 3′ adapter. Ligation products were amplified, purified and subjected to sequencing using the Illumina HiSeq 2000.

Bioinformatics analysis

For small RNA sequencing data, the raw reads were first filtered by removing low-quality reads, including reads with a length <18 nt, a poly-A sequence, a 5′ adapter or no 3′ adapter and no insert tag, to obtain clean reads (sRNAs). All sRNAs were then aligned to the cotton genome [*G. hirsutum* TM-1 (AD)1] (Zhang *et al.*, 2015) to obtain tag expression and genomic location information, including repeat, intron and exon site annotation using the Short Oligonucleotide Analysis Package (SOAP). The sRNAs were then aligned to the GenBank (ftp://ftp.ncbi.nlm.nih.gov/genbank/) and Rfam 11.0 (http://rfam.janelia.org/) databases to annotate the rRNA, tRNA, small cytoplasmic RNA (scRNA), small nuclear RNA (snRNA) and small nucleolar RNA (snoRNA). All associated tags (repeat, intron, exon, rRNA, tRNA, scRNA, snRNA or snoRNA) were removed in subsequent miRNA analyses. Unannotated sRNAs were then used to predict secondary structure

using miReap combined with genome mapping information. The sRNAs with classic miRNA secondary structure were then aligned to the miRBase 21.0 (http://www.mirbase.org/ftp.shtml) to identify known miRNAs using miReap (http://sourceforge.net/projects/mireap/). In addition, sRNAs containing classic miRNA secondary structure but not mapped to miRbase were predicted to be novel miRNAs. The clean reads for each miRNA were normalized using the following formula: normalized expression (TPM) = mapped read count/total reads * 1 000 000. miRNA expression fold changes between samples were calculated using $\log_2$(TPM of sample 1/TPM of sample 2); two biological replicates were merged into mean value. The miRNA targets were predicted using the software psRobot and TargetFinder.

For the degradome sequencing data, the raw reads were first preprocessed using a Perl script to remove the reads with adapters, that were of low quality or that had an unknown base N to obtain clean tags. Among the clean tag sequences containing a single base, more than 70% were identified as polyN tags. Clean tags were aligned to the GenBank and Rfam 11.0 databases to get annotation information for the rRNA, tRNA, scRNA, snRNA and snoRNA, and were mapped to the cotton [(*G. hirsutum* TM-1 (AD) 1]) genome to obtain cDNA sense and antisense tags using SOAP 2.20. The tags mapped to cDNA or mRNA sequences were then used to predict cleavage sites. To predict the cleavage sites of targets, two software programs were used: PAREsnip (http://srna-workbench.cmp.uea.ac.uk/tools/paresnip/) was used to predict miRNA targets and perform hypothesis testing; and CleaveLand 3 (http://axtell-lab-psu.weebly.com/cleaveland.html) was used to summarize the information of cleaved sites, define categories (containing 0–5 categories) and plot T-plot figures. Gene function annotation and T-plot figures were created to show the function and cleavage sites of predicted miRNA targets.

RLM-RACE analysis

RNA ligase-mediated rapid amplification of cDNA ends was used to verify the accuracy of target cleavage sites detected from degradome sequence data. GeneRacer kit (Invitrogen, California, CA, USA) was used; briefly, the protocol is as follows: (1) total RNA (5 μg) from equal mixtures of all samples (16 samples containing biological repeats) was ligated to an RNA adapter without calf intestinal phosphatase treatment; (2) cDNA was transcribed by GeneRacer OligodT primers; (3) PCR was performed with 5′ adapter primers (sequence provided by manufacturer's instructions) and 3′ gene-specific primers (designed by Primer 5.0 and synthesized by Genscript, Nanjing, China); (4) PCR products were ligated to a T-easy vector (Promega, Madison, WI, USA) and sequenced by Tianyi Huiyuan (Wuhan, China).

Exogenous IAA application for 84021 and H05 under NT and HT stress

84021 and H05 cotton plants were grown under normal conditions (see above) until flowering. For IAA treatments, 1×10^{-6} mol L^{-1} IAA was sprayed on the cotton buds at night (to avoid degradation of IAA by light) every 2 days. The IAA treatment was applied for 7 days under NT conditions, after which the plants were moved to the HT conditions until male sterility appeared. At the same time, control plants (Mock) were placed under the same conditions, with the exception of being sprayed with IAA solvent on their buds. Anther samples were harvested according to the methods described above for RNA extraction and later for investigation of miRNA and gene expression levels. Buds from different developmental stages were fixed in FAA [10% formalin, 5% acetic acid and 50% alcohol (v/v)] for histological observation.

Histological observation

Histological observation was carried out to identify the response difference of 84021 and H05 to HT stress and IAA treatment, and to determine the relationship between bud length and anther developmental stage in miR157 transgenic cotton lines. Detailed methods have been described in previous reports (Deng *et al.*, 2012). Samples were stained with toluidine blue and then cut into 10-μm cross-sections. Photographs were then captured by an optical microscope (ZEISS Axioscope. A1, Jena, Germany).

qRT-PCR analysis

Stem-loop RT-PCR was used to quantify the expression levels of miRNAs and target genes according to previous studies (Varkonyi-Gasic *et al.*, 2007). In brief, 2 μg of total RNA mixed with 0.05 μM stem-loop primers, 2.5 μM Oligo dT primer, 0.4 μM dNTP and appropriate RNA-free water was incubated at 65°C for 5 min and then transferred to ice for 2 min. The mixture was then added to 4 μl of 5 × first-strand buffer, 1 μl of dithiothreitol (100 mM), 1 μl of RNaseOUT (40 units μl^{-1}) and 1 μl of SuperScript III RT (200 units μl^{-1}) in a 20- μl reaction. The reaction mixture was then reverse-transcribed using the following steps: 16°C for 30 min; 60 cycles of 30°C for 30 s, 42°C for 30 sec and 50°C for 1 s; and then 85°C for 5 min to inactivate the reverse transcriptase.

Quantitative reverse transcription PCR (qRT-PCR) was performed with 10 μl of 50 × diluted cDNA products, 10 μl of SsoFast EvaGreen Supermix With Low ROX (Bio-Rad, Hercules, CA, USA), and 0.25 μM forward and reverse primers using a 7500 real-time system (Applied Biosystems, Waltham, MA, USA). Ubiquitin7 (GhUBQ7) was used as the endogenous reference gene according to previous reports (Tu *et al.*, 2007). Relative miRNA or gene expression levels were calculated using the $2^{-\triangle Cr}$ method and primers used in this study listed in Table S5.

ACCESSION NUMBERS

The GenBank accession numbers for data of small RNA sequencing referred to in this paper are PRJNA393079

CONFLICT OF INTEREST

The authors declare no conflict of interest.

SUPPORTING INFORMATION

Additional Supporting Information may be found in the online version of this article.
Figure S1. Growth curve of cotton buds under NT.
Figure S2. Phylogenetic analysis of ARF gene members in *Gossypium hirsutum* and Arabidopsis.
Figure S3. The histological observation and the expression detection of *Cals5* in TS anthers of miR160 OE line and null control under NT and HT conditions.
Figure S4. The relative expression level of genes related to JA biosynthesis. *GhUB7* was used as the control.
Figure S5. Plant phenotype and the relationship between bud length and anther developmental stages of miR157 transgenic lines.

Table S1. Total reads and normalized expression level of identified known and novel miRNAs in 16 samples (miRNAs with bold front means reads less than 20 or TPM less than 10 in all samples).

Table S2. Reads and percentage of conserved and non-conserved miRNA families and novel miRNAs with TPM >10 in each sample.

Table S3. Total reads and annotation information for degradome sequencing.

Table S4. Target gene and predicted cleavage site information validated through degradome sequencing.

Table S5. The primers used in this study.

REFERENCES

Addo-Quaye, C., Eshoo, T.W., Bartel, D.P. and Axtell, M.J. (2008) Endogenous siRNA and miRNA targets identified by sequencing of the Arabidopsis degradome. *Curr. Biol.* **18**, 758–762.

Ahmed, F.E., Hall, A.E. and DeMason, D.A. (1992) Heat injury during floral development in Cowpea (Vigna unguiculata, Fabaceae). *Am. J. Bot.* **79**, 784–791.

Bingham, J. (1966) Varietal response in wheat to water supply in the field, and male sterility caused by a period of drought in a glasshouse experiment. *Ann. Appl. Biol.* **57**, 365–377.

Bita, C.E. and Gerats, T. (2013) Plant tolerance to high temperature in a changing environment: scientific fundamentals and production of heat stress-tolerant crops. *Front. Plant Sci.* **4**, 273.

Bokszczanin, K.L., Fragkostefanakis, S. and Thermotolerance, S.P. (2013) Perspectives on deciphering mechanisms underlying plant heat stress response and thermotolerance. *Front. Plant. Sci.* **4**, 315.

Cecchetti, V., Altamura, M.M., Brunetti, P., Petrocelli, V., Falasca, G., Ljung, K., Costantino, P. and Cardarelli, M. (2013) Auxin controls Arabidopsis anther dehiscence by regulating endothecium lignification and jasmonic acid biosynthesis. *Plant J.* **74**, 411–422.

Chen, L.T. and Liu, Y.G. (2014) Male sterility and fertility restoration in crops. *Annu. Rev. Plant Biol.* **65**, 579–606.

Chen, R., Zhao, X., Shao, Z., Wei, Z., Wang, Y., Zhu, L., Zhao, J., Sun, M., He, R. and He, G. (2007) Rice UDP-glucose pyrophosphorylase1 is essential for pollen callose deposition and its cosuppression results in a new type of thermosensitive genic male sterility. *Plant Cell*, **19**, 847–861.

Cheng, Y.F., Dai, X.H. and Zhao, Y.D. (2006) Auxin biosynthesis by the YUCCA flavin monooxygenases controls the formation of floral organs and vascular tissues in Arabidopsis. *Gene Dev.* **20**, 1790–1799.

Chhun, T., Aya, K., Asano, K., Yamamoto, E., Morinaka, Y., Watanabe, M., Kitano, H., Ashikari, M., Matsuoka, M. and Ueguchi-Tanaka, M. (2007) Gibberellin regulates pollen viability and pollen tube growth in rice. *Plant Cell*, **19**, 3876–3888.

Cuperus, J.T., Fahlgren, N. and Carrington, J.C. (2011) Evolution and functional diversification of MIRNA genes. *Plant Cell*, **23**, 431–442.

De Storme, N. and Geelen, D. (2014) The impact of environmental stress on male reproductive development in plants: biological processes and molecular mechanisms. *Plant, Cell Environ.* **37**, 1–18.

Deng, F.L., Tu, L.L., Tan, J.F., Li, Y., Nie, Y.C. and Zhang, X.L. (2012) GbPDF1 is involved in cotton fiber initiation via the core cis-element HDZIP2A-TATHB2. *Plant Physiol.* **158**, 890–904.

Devoto, A., Nieto-Rostro, M., Xie, D., Ellis, C., Harmston, R., Patrick, E., Davis, J., Sherratt, L., Coleman, M. and Turner, J.G. (2002) COI1 links jasmonate signalling and fertility to the SCF ubiquitin-ligase complex in Arabidopsis. *Plant J.*, **32**, 457–466.

Endo, M., Tsuchiya, T., Hamada, K., Kawamura, S., Yano, K., Ohshima, M., Higashitani, A., Watanabe, M. and Kawagishi-Kobayashi, M. (2009) High temperatures cause male sterility in rice plants with transcriptional alterations during pollen development. *Plant Cell Physiol.* **50**, 1911–1922.

German, M.A., Luo, S.J., Schroth, G., Meyers, B.C. and Green, P.J. (2009) Construction of Parallel Analysis of RNA Ends (PARE) libraries for the study of cleaved miRNA targets and the RNA degradome. *Nat. Protoc.* **4**, 356–362.

Guan, Q., Lu, X., Zeng, H., Zhang, Y. and Zhu, J. (2013) Heat stress induction of miR398 triggers a regulatory loop that is critical for thermotolerance in Arabidopsis. *Plant J.*, **74**, 840–851.

Huang, Z., Shi, T., Zheng, B., Yumul, R.E., Liu, X., You, C., Gao, Z., Xiao, L. and Chen, X. (2016) APETALA2 antagonizes the transcriptional activity of AGAMOUS in regulating floral stem cells in Arabidopsis thaliana. *New Phytol.* (Epub ahead of print). Available at: https://doi.org/10.1111/nph.14151.

Kim, S.Y., Hong, C.B. and Lee, I. (2001) Heat shock stress causes stage-specific male sterility in Arabidopsis thaliana. *J. Plant. Res.* **114**, 301–307.

Kim, J.J., Lee, J.H., Kim, W., Jung, H.S., Huijser, P. and Ahn, J.H. (2012) The miR156-SPL3 module regulates ambient temperature-responsive flowering via FT in Arabidopsis thaliana. *Plant Physiol.* **159**, 461–478.

Kruszka, K., Pacak, A., Swida-Barteczka, A., Nuc, P., Alaba, S., Wroblewska, Z., Karlowski, W., Jarmolowski, A. and Szweykowska-Kulinska, Z. (2014) Transcriptionally and post-transcriptionally regulated microRNAs in heat stress response in barley. *J. Exp. Bot.* **65**, 6123–6135.

Li, M.Y., Wang, F., Xu, Z.S., Jiang, Q., Ma, J., Tan, G.F. and Xiong, A.S. (2014) High throughput sequencing of two celery varieties small RNAs identifies microRNAs involved in temperature stress response. *BMC Genom.* **15**, 242.

Li, W., Wang, T., Zhang, Y. and Li, Y. (2016) Overexpression of soybean miR172c confers tolerance to water deficit and salt stress, but increases ABA sensitivity in transgenic Arabidopsis thaliana. *J. Exp. Bot.* **67**, 175–194.

Liu, N., Tu, L., Tang, W., Gao, W., Lindsey, K. and Zhang, X. (2014) Small RNA and degradome profiling reveals a role for miRNAs and their targets in the developing fibers of Gossypium barbadense. *Plant J.* **80**, 331–344.

Liu, N., Tu, L., Wang, L., Hu, H., Xu, J. and Zhang, X. (2017) MicroRNA 157-targeted SPL genes regulate floral organ size and ovule production in cotton. *BMC Plant Biol.* **17**, 7.

Matzke, M.A. and Mosher, R.A. (2014) RNA-directed DNA methylation: an epigenetic pathway of increasing complexity. *Nat. Rev. Genet.* **15**, 394–408.

Min, L., Zhu, L., Tu, L., Deng, F., Yuan, D. and Zhang, X. (2013) Cotton GhCKI disrupts normal male reproduction by delaying tapetum programmed cell death via inactivating starch synthase. *Plant J.* **75**, 823–835.

Min, L., Li, Y.Y., Hu, Q., Zhu, L.F., Gao, W.H., Wu, Y.L., Ding, Y.H., Liu, S.M., Yang, X.Y. and Zhang, X.L. (2014) Sugar and auxin signaling pathways respond to high-temperature stress during anther development as revealed by transcript profiling analysis in cotton. *Plant Physiol.* **164**, 1293–1308.

Namuco, O.S. and O'Toole, J.C. (1986) Reproductive stage water stress and sterility. I. Effect of stress during meiosis1. *Crop Sci.* **26**, 317–321.

Nizampatnam, N.R., Schreier, S.J., Damodaran, S., Adhikari, S. and Subramanian, S. (2015) microRNA160 dictates stage-specific auxin and cytokinin sensitivities and directs soybean nodule development. *Plant J.* **84**, 140–153.

Nova-Franco, B., Iniguez, L.P., Valdes-Lopez, O. et al. (2015) The microRNA172c-APETALA2-1 node as a key regulator of the common bean-Rhizobium etli nitrogen fixation symbiosis. *Plant Physiol.* **168**, 273–U502.

Okushima, Y., Overvoorde, P.J., Arima, K. et al. (2005) Functional genomic analysis of the AUXIN RESPONSE FACTOR gene family members in Arabidopsis thaliana: unique and overlapping functions of ARF7 and ARF19. *Plant Cell*, **17**, 444–463.

Paupiere, M.J., van Heusden, A.W. and Bovy, A.G. (2014) The metabolic basis of pollen thermo-tolerance: perspectives for breeding. *Metabolites*, **4**, 889–920.

Saini, H., Sedgley, M. and Aspinall, D. (1984) Development anatomy in wheat of male sterility induced by heat stress, water deficit or abscisic acid. *Funct. Plant Biol.* **11**, 243–253.

Sakata, T., Oshino, T., Miura, S., Tomabechi, M., Tsunaga, Y., Higashitani, N., Miyazawa, Y., Takahashi, H., Watanabe, M. and Higashitani, A. (2010) Auxins reverse plant male sterility caused by high temperatures. *Proc. Natl Acad. Sci. USA*, **107**, 8569–8574.

Sanders, M.P., Bui, Q.A., Weterings, K., McIntire, N.K., Hsu, Y.-C., Lee, Y.P., Truong, T.M., Beals, P.T. and Goldberg, B.R. (1999) Anther developmental defects in Arabidopsis thaliana male-sterile mutants. *Sexual Plant Reprod.* **11**, 297–322.

Sanders, P.M., Lee, P.Y., Biesgen, C., Boone, J.D., Beals, T.P., Weiler, E.W. and Goldberg, R.B. (2000) The arabidopsis DELAYED DEHISCENCE1 gene

encodes an enzyme in the jasmonic acid synthesis pathway. *Plant Cell*, **12**, 1041–1061.

Sato, S., Peet, M.M. and Thomas, J.F. (2002) Determining critical pre- and post-anthesis periods and physiological processes in Lycopersicon esculentum Mill. exposed to moderately elevated temperatures. *J. Exp. Bot.* **53**, 1187–1195.

Shi, Z.H., Zhang, C., Xu, X.F., Zhu, J., Zhou, Q., Ma, L.J., Niu, J. and Yang, Z.N. (2015) Overexpression of AtTTP affects ARF17 expression and leads to male sterility in Arabidopsis. *PLoS ONE*, **10**, e0117317.

Stief, A., Altmann, S., Hoffmann, K., Pant, B.D., Scheible, W.-R. and Baeurle, I. (2014) Arabidopsis miR156 regulates tolerance to recurring environmental stress through SPL transcription factors. *Plant Cell*, **26**, 1792–1807.

Sun, G. (2012) MicroRNAs and their diverse functions in plants. *Plant Mol. Biol.* **80**, 17–36.

Tang, J.H., Fu, Z.Y., Hu, Y.M., Li, J.S., Sun, L.L. and Ji, H.Q. (2006) Genetic analyses and mapping of a new thermo-sensitive genic male sterile gene in maize. *Theor. Appl. Genet.* **113**, 11–15.

Tu, L., Zhang, X., Liu, D., Jin, S., Cao, J., Zhu, L., Deng, F., Tan, J. and Zhang, C. (2007) Suitable internal control genes for qRT-PCR normalization in cotton fiber development and somatic embryogenesis. *Chinese Sci. Bull.* **52**, 3110–3117.

Varkonyi-Gasic, E., Wu, R., Wood, M., Walton, E.F. and Hellens, R.P. (2007) Protocol: a highly sensitive RT-PCR method for detection and quantification of microRNAs. *Plant Meth.* **3**, 12.

Vernoux, T., Brunoud, G., Farcot, E. *et al.* (2011) The auxin signalling network translates dynamic input into robust patterning at the shoot apex. *Mol. Syst. Biol.* **7**, 508.

Wang, J.W., Wang, L.J., Mao, Y.B., Cai, W.J., Xue, H.W. and Chen, X.Y. (2005) Control of root cap formation by MicroRNA-targeted auxin response factors in Arabidopsis. *Plant Cell*, **17**, 2204–2216.

Wang, Z.S., Wang, Y., Kohalmi, S.E., Amyot, L. and Hannoufa, A. (2016) SQUAMOSA PROMOTER BINDING PROTEIN-LIKE 2 controls floral organ development and plant fertility by activating ASYMMETRIC LEAVES 2 in Arabidopsis thaliana. *Plant Mol. Biol.* **92**, 661–674.

Wollmann, H., Mica, E., Todesco, M., Long, J.A. and Weigel, D. (2010) On reconciling the interactions between APETALA2, miR172 and AGAMOUS with the ABC model of flower development. *Development*, **137**, 3633–3642.

Wu, M.F., Tian, Q. and Reed, J.W. (2006) Arabidopsis microRNA167 controls patterns of ARF6 and ARF8 expression, and regulates both female and male reproduction. *Development*, **133**, 4211–4218.

Wu, Y., Min, L., Wu, Z., Yang, L., Zhu, L., Yang, X., Yuan, D., Guo, X. and Zhang, X. (2015) Defective pollen wall contributes to male sterility in the male sterile line 1355A of cotton. *Sci. Rep.* **5**, 9608.

Xing, Q.H., Ru, Z.G., Zhou, C.J., Xue, X., Liang, C.Y., Yang, D.E., Jin, D.M. and Wang, B. (2003) Genetic analysis, molecular tagging and mapping of the thermo-sensitive genic male-sterile gene (wtms1) in wheat. *Theor. Appl. Genet.* **107**, 1500–1504.

Xing, S.P., Salinas, M., Hohmann, S., Berndtgen, R. and Huijser, P. (2010) miR156-targeted and nontargeted SBP-box transcription factors act in concert to secure male fertility in Arabidopsis. *Plant Cell*, **22**, 3935–3950.

Xing, S.P., Salinas, M., Garcia-Molina, A., Hohmann, S., Berndtgen, R. and Huijser, P. (2013) SPL8 and miR156-targeted SPL genes redundantly regulate Arabidopsis gynoecium differential patterning. *Plant J.* **75**, 566–577.

Yang, J., Tian, L., Sun, M.X., Huang, X.Y., Zhu, J., Guan, Y.F., Jia, Q.S. and Yang, Z.N. (2013) AUXIN RESPONSE FACTOR17 is essential for pollen wall pattern formation in Arabidopsis. *Plant Physiol.* **162**, 720–731.

Yasuor, H., Abu-Abied, M., Belausov, E., Madmony, A., Sadot, E., Riov, J., Rubin, B. (2006) Glyphosate-induced anther indehiscence in cotton is partially temperature dependent and involves cytoskeleton and secondary wall modifications and auxin accumulation. *Plant Physiol.* **141**, 1306–1315.

Ye, Q.Q., Zhu, W.J., Li, L., Zhang, S.S., Yin, Y.H., Ma, H. and Wang, X.L. (2010) Brassinosteroids control male fertility by regulating the expression of key genes involved in Arabidopsis anther and pollen development. *Proc. Natl Acad. Sci. USA*, **107**, 6100–6105.

Yu, N., Niu, Q.W., Ng, K.H. and Chua, N.H. (2015) The role of miR156/SPLs modules in Arabidopsis lateral root development. *Plant J.* **83**, 673–685.

Zeng, X., Li, W., Wu, Y. *et al.* (2014) Fine mapping of a dominant thermo-sensitive genic male sterility gene (BntsMs) in rapeseed (Brassica napus) with AFLP- and Brassica rapa-derived PCR markers. *Theor. Appl. Genet.* **127**, 1733–1740.

Zhai, Q., Zhang, X., Wu, F., Feng, H., Deng, L., Xu, L., Zhang, M., Wang, Q. and Li, C. (2015) Transcriptional mechanism of jasmonate receptor COI1-mediated delay of flowering time in Arabidopsis. *Plant Cell*, **27**, 2814–2828.

Zhang, B. (2015) MicroRNA: a new target for improving plant tolerance to abiotic stress. *J. Exp. Bot.* **66**, 1749–1761.

Zhang, T., Hu, Y., Jiang, W. *et al.* (2015) Sequencing of allotetraploid cotton (Gossypium hirsutum L. acc. TM-1) provides a resource for fiber improvement. *Nat. Biotechnol.* **33**, 531–537.

Zhao, Z., Zhang, Y., Liu, X. *et al.* (2013) A role for a dioxygenase in auxin metabolism and reproductive development in rice. *Dev. Cell*, **27**, 113–122.

Zhao, J., He, Q., Chen, G., Wang, L. and Jin, B. (2016) Regulation of non-coding RNAs in heat stress responses of plants. *Front. Plant Sci.* **7**, 1213.

Zhi, L.I.U., Shaoqing, L.I.U., Xiaonan, Y.U. and Jinxiang, C. (2007) Response of fertile pollen grains to different temperatures and cytological base of male sterility in TemianS-1. *J. Hum. Agricult. Univ.* **33**, 403–406.

Zhu, L.T.L., Zeng, F., Liu, D. and Zhang, X. (2005) An improved simple protocol for isolation of high quality RNA from Gossypium spp. suitable for cDNA library construction. *Acta Agron. Sin.* **31**, 1657–1659.